Neurology Asia 2022; 27(4) : 819 – 833

VIEWS AND REVIEW

Neuroimaging in dementia syndromes

[1]Kartini Rahmat, [1]Affendi Haris Phuah, [1]Norlisah Ramli, [1]Nadia Fareeda Muhammad Gowdh, [1]Wai Yee Chan, [2]Maw Pin Tan

[1]Department of Biomedical Imaging, [2]Division of Geriatrics, Department of Medicine, Faculty of Medicine, Universiti Malaya, Kuala Lumpur, Malaysia

Abstract

Neuroimaging is essential for early diagnosis of different types of dementia. Structural imaging is recommended for patients with new-onset cognitive impairment and magnetic resonance imaging is the modality of choice. When atypical features are present, functional and molecular imaging is helpful for further characterisation of neurodegenerative changes. Accurate identification of dementia subtypes enables early initiation of specific molecular targeted therapies. This article provides an overview of the structural, biochemical and functional changes in common dementia subtypes that may be diagnosed through neuroimaging, emphasising new techniques like perfusion and functional imaging.

Keywords: Dementia, magnetic resonance imaging (MRI), perfusion imaging, functional imaging, cognitive dysfunction

INTRODUCTION

Dementia is a chronic and progressive mental disorder resulting in an impaired ability to perform daily activities. Patients experience cognitive and physical impairments, including memory loss, personality changes and altered perception.[1] The likelihood of developing dementia increases with age, hence its prevalence among the elderly and the rising prevalence as life expectancy increases.

There are several common dementia subtypes caused by different pathophysiology, with the most common being Alzheimer's disease (AD).[2] At the time of diagnosis, the neuropathological damage is likely to be extensive and irreversible; thus, structural imaging via magnetic resonance imaging (MRI) and functional imaging are vital in identifying dementia changes early to initiate appropriate therapy to arrest further cognitive decline.[3]

This review focuses on imaging findings of common dementia syndromes related to structural, biochemical and functional changes. Reversible causes of cognitive impairment are not discussed in this article.

INDICATIONS FOR IMAGING

Patients with new-onset cognitive impairment should be investigated with at least one brain imaging modality, either computer tomography (CT) or MRI.[3] In addition, repeat imaging is sometimes necessary to assess disease progression and document treatment response. The MRI neurodegenerative or dementia protocol typically includes sequences as below:

1. Coronal oblique T1W imaging for assessing the medial temporal lobe and hippocampus of the brain;
2. Fluid-attenuated inversion recovery (FLAIR) and T2 FSE sequences to detect vascular pathology, infarctions and global cortical atrophy;
3. Axial susceptibility-weighted imaging (SWI) or T2* gradient-echo for detection of micro-bleeds or superficial siderosis;
4. Diffusion-Weighted Imaging (DWI) for detecting underlying vasculitis and prion infection, i.e. Creutzfeldt-Jakob disease;
5. (Optional) Perfusion Imaging, including Arterial Spin Labelling (ASL) to provide additional information on cerebrovascular integrity; and,
6. (Optional) Diffusion Tensor Imaging (DTI) to evaluate the integrity of white matter tracts.

The isovoxel T1-weighted (T1W) and T2/FLAIR sequences are necessary to assess brain structure and signalling changes. The MRI brain dementia protocol used at our institution (which has a 3.0 Tesla scanner) is stated in Table 1.

Address correspondence to: Nadia Fareeda Muhammad Gowdh, Department of Biomedical Imaging, Faculty of Medicine, Universiti Malaya, 50603 Kuala Lumpur, Malaysia. Tel: +60173541551 (mobile), +60379492091 (office). Email: nadia_fareeda@ummc.edu.my

Date of Submission: 14 December 2021; Date of Acceptance: 10 August 2022

https://doi.org/10.54029/2022aym

Table 1: Standard MRI brain dementia protocol with 3.0 Tesla at our institution

	T1 MPRAGE	T2W TSE	T2 TIRM Dark Fluid	DWI (RESOLVE)	SWI	MRA TOF
Spatial resolution, mm	256 x 100	512 x 75	320 x 70	224 x 100	256 x 96	384 x 95
FOV (mm)	230	230	220	230	220	200
TE/TR (ms)	2.48/ 2200	100/6000	81/9000	62/3800	20/27	3.43/21
Inversion time (ms)	900	N/A	2500	N/A	N/A	N/A
FA	8	150	150	180	15	18
Matrix	0.9 x 0.9	0.4 x 0.4	0.7 x 0.7	1.0 x 1.0	0.9 x 0.9	0.3 x 0.3
Slice thickness (mm)	1	4	4	4	1.5	0.5
Parallel imaging factor (GRAPPA)	2	N/A	2	2	2	2
Distance factor (mm)	50%	1.2	1.2	1.2	20%	-2.0
Scan duration (min)	5.38	1.56	2.44	2.53	4.54	5.59

MPRAGE Magnetization-prepared rapid gradient-echo; TIRM turbo inversion recovery magnitude; diffusionweighted imaging; susceptibility-weighted imaging; MRA TOF magnetic resonance imaging time of flight

The use of functional and molecular imaging is limited by cost and scanner availability. Dementia-related indicators for radioimaging cerebral metabolic studies, such as positron emission tomography with 2-deoxy-2-18F-fluorodeoxyglucose (FDG-PET) or perfusion techniques such as 99mTchexamethylpropyleneamine oxime (HMPAO), include:

- Circumstances in which the differential diagnosis is needed to differentiate between AD, dementia with Lewy bodies (DLB) and frontotemporal dementia;
- Cases of suspected AD in patients with mild cognitive impairment;
- Possible AD with persistent uncertainties about the diagnosis despite thorough evaluations;
- AD patients meet core criteria for dementia but have atypical presentations or unexpectedly early age of onset.

Ultrahigh-resolution imaging using 7T MRI allows better visualisation of microstructures and pathological changes typically involved in dementia pathologies such as plaques, microbleeds, and neurofibrillary tangles that were not previously visible on in vivo imaging. Image resolution increases as the B0 increases. Although the signal to noise ratio (SNR) increases with increasing B0, higher B0 is also more susceptible to field inhomogeneity and artefacts; thus, higher electromagnetic field imaging presents its own advantages and challenges.[4]

Diffusion tensor imaging

DTI evaluates white matter tract integrity to allow a three-direction quantitative evaluation of water diffusion in the brain (right/left, front/back, up/down), implying the degree of anisotropy and local fibre direction voxel by voxel. Fractional anisotropy (FA) measures diffusion directionality, whereas mean diffusivity (MD) provides a measure of translational diffusion, the average diffusion in all directions. Furthermore, diffusion along the direction of axonal fibres is reflected by axial diffusivity (AxD), while radial diffusivity (RD) reflects diffusion in a perpendicular direction.[5]

In cerebral white matter, diffusion along the axon direction is facilitated while perpendicular diffusion is impeded. When the white matter is damaged, free diffusion will increase, resulting in an increase in MD and a decrease in FA. Neurite orientation dispersion and density imaging (NODDI) is another neuronal diffusion parameter. NODDI is said to overcome the limitations of DTI and diffusion kurtosis imaging (DKI) as it allows tri-compartmental analysis. NODDI parameters include intracellular volume fraction (Vic) and the orientation dispersion (OD) index, which reflect neurite density and spatial configuration, respectively.[6]

Perfusion imaging

ASL perfusion MRI is a non-invasive technique to assess brain perfusion deficiencies without contrast medium or radioisotopes required in FDG–PET and HMPAO SPECT imaging. Functional MRI can also be performed by measuring blood oxygen level-dependent (BOLD) signals in the brain at a resting state and while performing mentally-challenging tasks.[7]

Functional imaging

Single-photon emission computed tomography (SPECT) and positron emission tomography (PET) are used to identify changes in brain physiology in dementia, notably metabolic abnormalities. Contrast medium and isotopes like [18F] fluorodeoxyglucose (FDG) in PET and 99mTchexamethylpropyleneamine oxime (HMPAO) in SPECT are often used to measure brain energy metabolism and study cerebral perfusion, respectively. Newer PET ligands for imaging disease-specific pathologies have the potential to improve brain imaging in neurodegenerative disease significantly. Compounds that bind to amyloid, including radiolabelled Pittsburgh compound B [(11C)PiB] and (18F)AV-45 (flobetapir F18), are available. Still, the prohibitive cost of these ligands has limited the use of amyloid PET scans in clinical practice. Flobetapir F18 has a longer half-life than PiB but has lower specificity for β-amyloid. In vivo imaging techniques for tau, an alternative biomarker for AD, and TDP-43 or α-synuclein for other neurodegenerative diseases remain elusive.

Network connectivity imaging

The integrity of the brain network is an integral component of normal brain function. Molecular changes may lead to neuropathology, disrupting normal connections and resulting in distinct disease manifestations. Brain connectivity can be assessed using functional MRI, electroencephalography and magnetoencephalography, and post-processing of structural imaging sequences such as diffusion tensor imaging and tractography. Distinct network disruption patterns have been found in major neurodegenerative diseases. This is especially useful in the AD and FTD subtypes of dementia. Tuladhar *et al*. found that those with worse network disruptions identified on DTI were associated with a higher risk of developing dementia among patients with small vessel disease. Network assessments using DTI were more helpful than structural changes such as lacunes, white matter hyperintensities and atrophy in this cohort.[8] Thus connectivity imaging has clinical implications of enabling more accurate diagnoses, early detection and monitoring of disease progression.[9]

ALZHEIMER'S DISEASE

AD is among the most common subtypes of dementia.[2] Patients usually experience progressive deterioration of episodic memory with minor language or visual processing difficulties. The pathology involves the deposition of two abnormal protein aggregates in brain tissue — amyloid plaques and neurofibrillary tangles.[10] Most patients have a pre-dementia stage, known as mild cognitive impairment (MCI). MCI is a state of accelerated cognitive decline for a person's age and education level without interference in daily activities.[11] The imaging findings in MCI often resemble that of AD. Hippocampal atrophy is a robust marker for the development of AD (Figure1).[12]

Early AD is typically associated with atrophy in the strata radiatum, lacunosum and moleculare subfields within the cornu ammonis layer 1 of the hippocampus (CA1-SRLM). Conventional 3T imaging can detect hippocampal substructure atrophy, specifically the CA1, CA2 and subiculum substructure atrophy in AD, better than 1.5T imaging.[12] Ultrahigh field imaging using 7T B0 enables further improved segmentation of hippocampal substructures and morphometric assessment of substructure volume. CA1-SRLM volume changes without total CA1 or total hippocampal width changes, likely very early AD changes, have only been detected on 7T imaging. Thus, 7T imaging may soon be clinically helpful to differentiate MCI and AD from controls.[4]

Focal cerebral volume loss typically starts in the entorhinal cortex, which progresses to the hippocampus, medial temporal cortex and

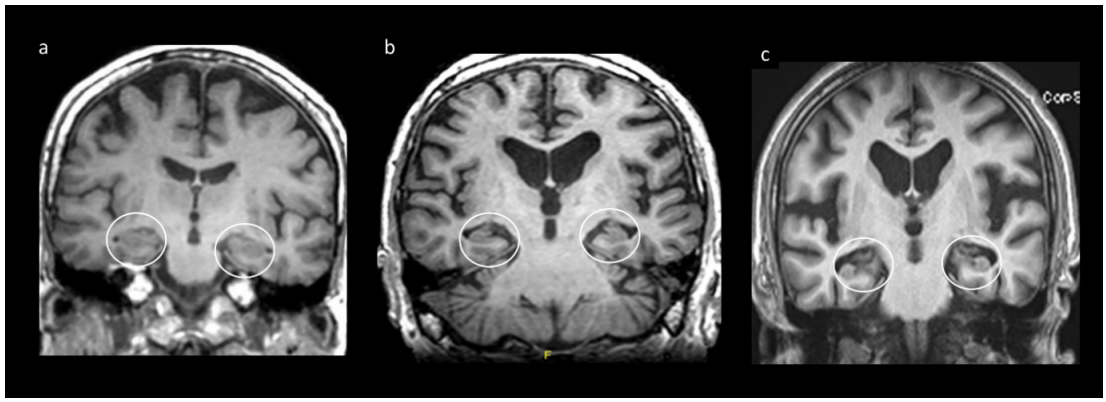

Figure 1. Medial temporal lobe appearances on magnetic resonance imaging in mild cognitive impairment and Alzheimer's disease.
T1W FSPGR coronal view of medial temporal lobes (circle) in a (a) normal study with no atrophy (medial temporal lobe atrophy (MTA) score 0), (b) Mild cognitive disorder with mild bilateral medial temporal atrophy (MTA score 2) and (c) Alzheimer's disease with moderate bilateral medial temporal atrophy (MTA score 3). These images depict the progressive medial temporal atrophy from normal to mild cognitive impairment and eventually Alzheimer's disease.

medial parietal lobe (Figure 2).[13] The degree of hippocampal atrophy is associated with clinical cognitive impairment. Less extensive atrophy may also be found in the left superior parietal lobule, left anterior cingulate gyrus and bilateral thalamus.[14]

Amyloid plaques are well-identified using PET with amyloid-bindings ligands. Amyloid

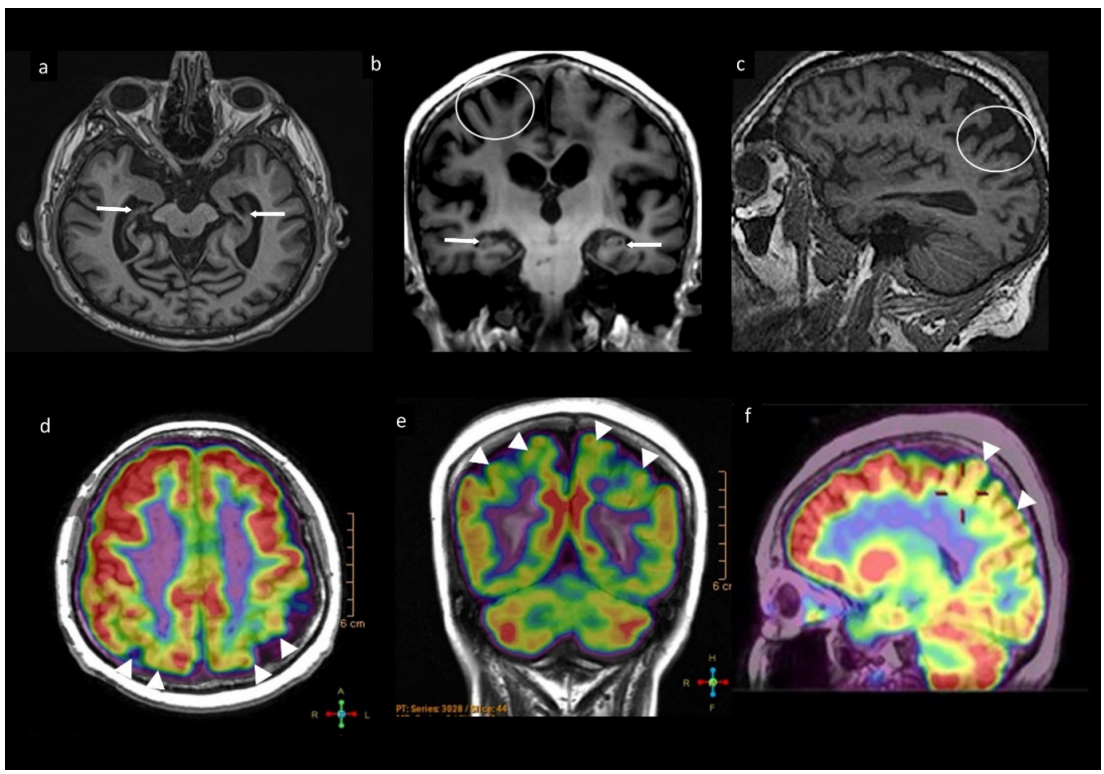

Figure 2. Alzheimer's disease
MRI reveals bilateral medial temporal lobe and hippocampal atrophy (arrows) on (a)axial and (b)coronal images. Precuneus atrophy (circle) is observed on the (b) coronal and (c) sagittal images. ^{18}FDG PET/MRI co-registered images (d)-(f) demonstrate decreased glucose metabolism (arrowhead) in the biparietal cortex, precuneus and posterior cingulate cortices.

plaques have high iron content, thus subjecting the tissue to higher susceptibility effects on MRI. Post-mortem studies correlating susceptibility effects on 7T MRI with histologic stains for iron reported that hypointensities were associated with amyloid deposits, microscopic iron and activated microglia.[15]

In AD, FA is reduced in the cingulum bundle that connects the hippocampus to the posterior cingulate region, medial temporal lobe subregions, including the hippocampus, entorhinal cortex and parahippocampal white matter and the actual temporal lobes.[16-21] Increased MD was found in the frontal[20,22], temporal[18], parietal and occipital lobes[16], parietal region of the superior longitudinal fasciculus[23], corpus callosum[22], cingulum[16], hippocampal and parahippocampal regions.[16] AxD and RD differences involving the corpus callosum (CC), temporal lobe, cingulum and hippocampal cingulum have been noted in AD patients.[5]

FDG PET and HMPAO SPECT have consistently demonstrated a reduction of cerebral metabolism and blood flow in the temporoparietal association cortex, in the posterior cingulate cortex and, to a lesser extent, in frontal association cortices with relative sparing of primary motor and sensory cortices in AD and MCI.[24] PiB is retained in the frontal, parietal, temporal and occipital cortices and the striatum of AD patients, which are areas where the protein aggregates are found in abundance.[25] Flobetapir F18 accumulates in the precuneus, frontal and temporal cortices.[26] Significant hypoperfusion on ASL imaging has been found in the region of the right inferior parietal cortex to bilateral posterior cingulate gyri, bilateral superior and middle frontal gyri and left inferior parietal lobe.[27]

AD has been associated with a lowered default-mode functional connectivity and decreased resting state in the brain's posterior cingulate cortex and hippocampus.[28] There is reduced deactivation of the default mode network involved in the processing of attention information, suggesting decreased resting state and adaptation of the default mode network compared to non-patients.[29] To a lesser extent, signal changes within the limbic networks on task-based fMRI utilising memory recall has been observed in people with AD and MCI.[29]

MILD COGNITIVE IMPAIRMENT

A combination of demographic traits, cognitive assessment scores, genetic and biological markers, and selected neuroimaging findings serve as critical indicators in predicting progression from MCI to AD.[30] Morphometric analysis of patients with MCI showed significant atrophy in the medial temporal lobe and less extensive atrophy involving the left superior parietal lobule, thalami, left anterior cingulate gyrus and temporal lobe.[30,31] Varatharajah *et al*. (2019) reported that the insula, superior frontal, inferior parietal, parahippocampal, medial orbitofrontal, caudal anterior cingulate, superior parietal, cingulate isthmus, pars triangularis, posterior cingulate and subiculum cortical thickness might serve as markers in MRI for predicting progression from MCI to AD.[30] Reduced glucose metabolism at the left angular, bilateral temporal, and bilateral cingulum (as detected through FDG-PET) was helpful. In addition, temporal lobe changes seen through PIB-PET are useful imaging markers.[30,31] Morphometric analysis of patients with MCI shows significant atrophy to a lesser extent compared to AD at the medial temporal lobes with a less extensive condition at the left superior parietal lobule, both thalami, left anterior cingulate gyrus and temporal lobes.[14]

A meta-analysis by Stebbins *et al*. (2009) comparing DTI findings found reduced FA values in the medial temporal lobe of individuals with AD, including the entorhinal cortex, hippocampal and parahippocampal white matter, temporal lobe proper and posterior cingulum and to a lesser degree, those with MCI.[32] Increased MD values have been reported in AD's frontal, temporal lobe, parietal, occipital lobes, superior longitudinal fasciculus, corpus callosum, cingulum, hippocampal and parahippocampal regions, with increased MD being negatively correlated with cognitive performance in both AD and MCI.[32] An increase in RD has been reported in AD at the frontal, temporal and parietal lobes.[33] Reduced FA in the cingulum bundle, which connects the hippocampus to the posterior cingulate region of the brain, was found in patients with AD and MCI.[16] MCI has been associated with hypoperfusion changes in bilateral parietal lobes, posterior cingulate cortex, precuneus, left occipital lobe, bilateral frontal and temporal lobes (Figure 3).[27,34,35]

Regional hypoperfusion in the inferior right parietal lobe has been demonstrated among individuals with MCI.[27] Cerebral blood flow patterns may vary between AD and MCI, as individuals with MCI may also progress to vascular dementia (VaD) and other dementia subtypes. Binnewijzend *et al*. (2013) found reduced perfusion at the precuneus, parietal

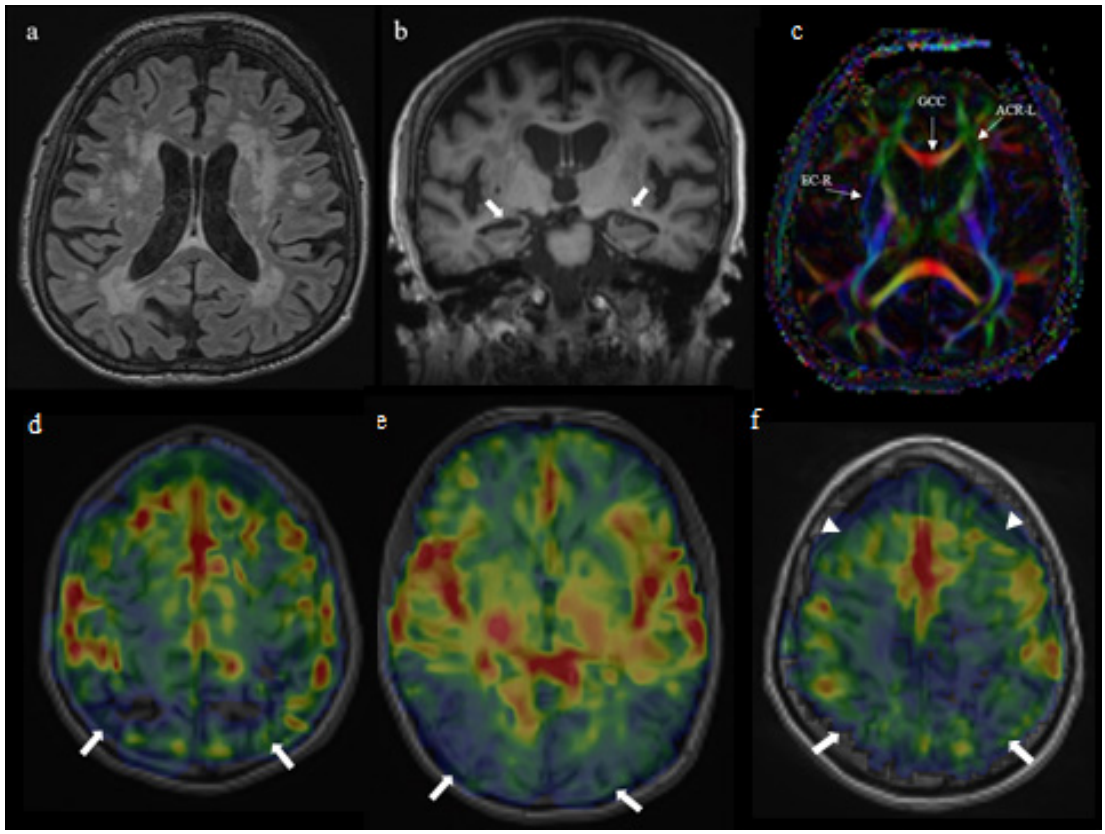

Figure 3. Mild cognitive impairment of mixed pathology – Vascular and AD pattern.
Magnetic resonance images: Bilateral deep and periventricular white matter lesions, Fazekas Grade 3 (a) with medial temporal lobe and hippocampal atrophy, MTA score 2 (b), FA colour map showing white matter tracts with significantly lower FA values in MCI patients compared to controls involving the genu of corpus callosum, left anterior corona radiata and right external capsule. Fused ASL Perfusion with T1W MRI brain images showing regional hypoperfusion at bilateral parietal lobes (white arrows-d), bilateral occipital lobes (white arrows –e), bilateral frontal lobes (arrowheads -f) and bilateral parietal lobes (white arrows –f).

and occipital lobes of patients with MCI.[34] Alexopoulos *et al*. (2012) found reduced perfusion in the parietal lobe, angular and middle temporal areas, left middle occipital lobe and precuneus to a lesser degree in MCI and AD.[36]

VASCULAR DEMENTIA

Vascular aetiology is the second most common cause of cognitive impairment among the older adults, with a high prevalence in males.[37] While a clinical diagnosis is usually made with memory and another cognitive dysfunction, the frontal-executive dysfunction predominates over the memory deficit. Large variations in brain appearance during imaging may be detected in VaD as the underlying neuropathology is cerebrovascular in origin. Hence, arteries of different sizes in different brain regions may be affected, and changes may also occur from ischemia or haemorrhage. Therefore, the neuroimaging appearances in vascular VaD may be classified as large vessel strokes, small vessel disease, and micro-haemorrhages.[38]

Single large vessel territory strokes typically involving the middle cerebral artery (MCA) territory of the dominant hemisphere or multiple smaller strokes in anterior cerebral arteries (ACA) or posterior cerebral artery (PCA) territories bilaterally have been found to be associated with 30% of cases with VaD.[39] Single smaller strokes may also lead to cognitive dysfunction if they occur in specific sites of the brain, such as the watershed territories, including the bilateral superior frontal gyrus or bilateral orbitofrontal (ACA/MCA) areas, the angular gyrus (ACA/MCA/PCA), the temporo-occipital junction and the inferior temporal gyrus.[40] Large infarcts tend

to have close temporal relation to the onset of dementia with a stepwise progression in cognitive decline.

Small vessel disease is the most commonly observed pathology in VaD. It occurs due to complete or incomplete infarcts in the white matter of subcortical grey matter nuclei.[41] The subcortical U-fibres and temporal lobes are usually spared in white matter infarcts.[42] Small infarcts can appear as focal T2-weighted hyperintense lacunes, hypointense on FLAIR or focal T2W/FLAIR hyperintense foci.[43] Several rating scales are helpful to assess the extent of white matter changes (WMC) in small vessel disease. The Fazekas scale, with only four classifications, is the most straightforward scale which can be used in clinical practice (Figure 3).

Another important neuroimaging aspect of VaD is micro-haemorrhages.[44] While macro-haemorrhages such as venous infarcts associated with cognitive impairment may be detected on[44] conventional T1- and T2-weighted spin-echo images, micro-haemorrhages are often challenging to identify on conventional sequences. They are better appreciated on T2*-weighted gradient-echo images. The aetiology is due to systemic hypertension.[45]

Diffusion-weighted imaging (DWI) may detect infarcts associated with acute onset dementia, otherwise known as strategic infarcts. This is increasingly recognised as an entity within a condition that is usually gradual and progressive. Compromised cerebral blood flow in small or large vessels may also be detected using MRI perfusion imaging. Arterial spin labelling provides additional information on cerebral blood flow (CBF), which is 20% lower in individuals with diffuse confluent white matter hyperintensities (WMH) compared to punctiform or early confluent WMH, hence adding to diagnostic certainties.[47]

FRONTOTEMPORAL LOBE DEGENERATION

Frontotemporal lobe degeneration (FTLD) occurs in younger individuals compared to AD and VaD.[48] There are three clinical syndromes of FTLD, specifically the behavioural variant frontotemporal dementia (BvFTD), semantic dementia (SD) and progressive non-fluent aphasia (PNFA). BvFTD is most associated with tau or TDP-43 protein deposition, while SD is most commonly found with TDP-43 and PNFA with tau and, to a lesser extent, TDP-43.[48] In FTLD, there is asymmetrical atrophy of the frontal and temporal cortices with relative sparing of the parietal and occipital lobes (Figure 4).[49] However, this may not be apparent on routine visual assessment on MRI. Increased T2W signal intensity may involve the subcortical white matter in the frontal and/or temporal regions.[50] In addition, there may be atrophy of the anterior or entire corpus callosum, which helps differentiate FTLD from AD, in which posterior corpus callosum atrophy predominates.[51] These observations may be refined in quantitative MRI, using either manual methods or voxel-based morphometry (VBM).[52]

BvFTD often manifests with symmetric frontal lobe atrophy, although asymmetric atrophy patterns predominantly involving the right frontal and right temporal lobe may occur.[49,53] In SD, there is typically atrophy in the left anterior inferior temporal lobe (with knife-edge type gyri), affecting the fusiform gyrus particularly. However, the entire left temporal lobe may be involved.[52] In addition, there is often involvement of the ventromedial and superior frontal lobes, and eventually, the right temporal lobe may also show a less-marked degree of volume loss. Finally, in PNFA, selective left perisylvian and frontal atrophy may occur.[43]

Alzheimer's disease may present with disproportionate and prominent impairment of frontal lobe functions in the early stages. Thus, functional neuroimaging (i.e., PET and SPECT) is useful to differentiate AD from FTLD.[53] Specific clinical syndromes are associated with particular hypometabolism patterns. Frontal hypometabolism is associated with BvFTD, left perisylvian with PNFA and temporal with SD.[53] On SPECT imaging, hypoperfusion at the anterior temporal and frontal lobes is more likely to be seen in FTLD rather than AD.[53] DTI can demonstrate the involvement of specific white matter tracts in various subtypes of FTLD. Widespread changes in the white matter have been reported in BvFTD, especially involving the anterior tracts, including the uncinate fasciculus, inferior longitudinal fasciculus and anterior commissural fibres.[54] PET neuroimaging using protein-specific radiolabelled ligands like 1C-PIB is very useful in distinguishing between the frontal variant of AD from FTLD.[55]

Perfusion MRI using the ASL technique may also help distinguish the presence of FTD. The combination of preserved parietal perfusion with decreased frontal perfusion differentiates BvFTD from AD with 87 % accuracy.[56] Damage to the inferior longitudinal fasciculus, uncinate fasciculus tracts in SD, and left superior

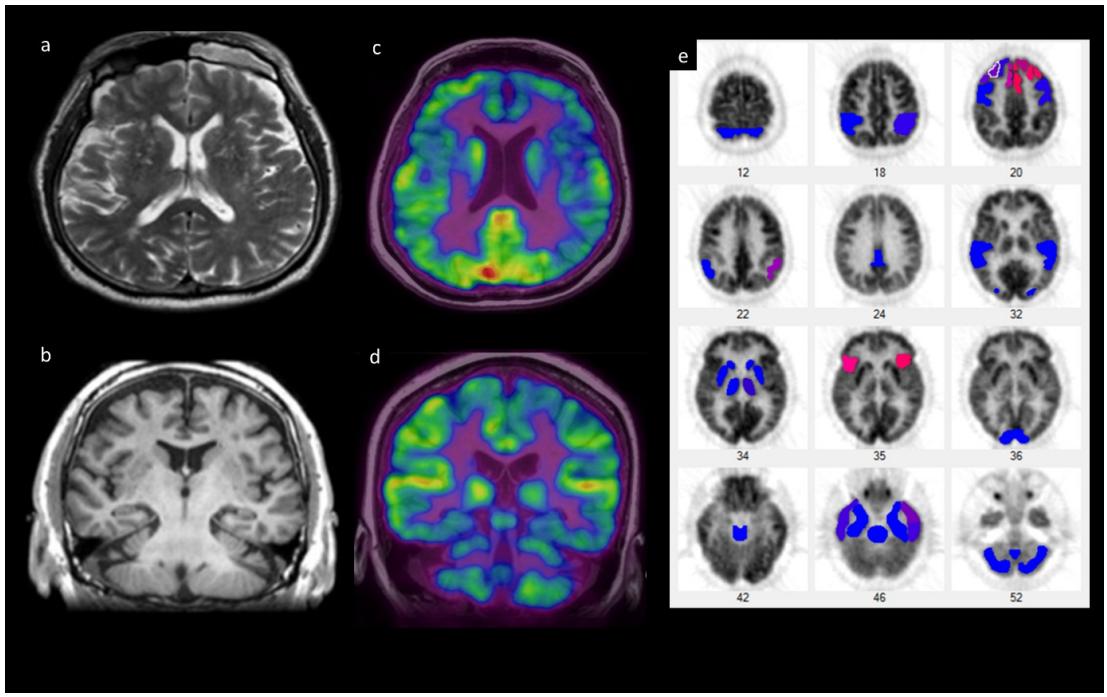

Figure 4. Frontotemporal dementia (FTD)
Magnetic resonance images: Bilateral frontal and temporal lobe atrophy is observed in the (a) axial image and medial temporal and hippocampal atrophy in (b) coronal image.
18FDG PET/ MRI co-registered images demonstrate decreased glucose metabolism, more pronounced in the bifrontal cortex, temporal lobes and hippocampus (c, d). In addition, the NeuroQ Analysis map showed reduced metabolism in the previously mentioned areas (e).

longitudinal fasciculus and anterior thalamic radiations were observed in PNFA.[57]

Functional MRI does have an emerging role in the diagnosis of FTLD. Reduced activity within the "Salience Network" during resting-state activity has been found on fMRI in BvFTD. This large-scale network includes the anterior cingulate and frontoinsular cortices, which are involved in the interpretation of social cognition.[58] In a separate study, task-based fMRI using non-verbal sounds showed different brain activation patterns within the superior temporal cortex in SD compared with healthy individuals.[43]

DEMENTIA WITH LEWY BODIES (DLB)

Lewy bodies are intracellular pathological aggregations of alpha synuclein, which can be found in the cortex, brainstem and substantia nigra.[38] Dementia with Lewy bodies (DLB) is characterised by cognitive impairment with executive dysfunction, visuospatial impairment, visual hallucinations, Parkinsonian motor features, fluctuations in cognition and arousal, rapid eye movement disorder and severe neuroleptic sensitivity. These features may overlap between DLB and Parkinson's disease. DLB is diagnosed if the dementia symptoms precede the motor symptoms or become apparent within 12 months of the motor symptoms.[59] Imaging findings in DLB include global and subcortical volume loss with relative preservation of the hippocampi (Figure 5).[60] However, medial temporal lobe atrophy does not exclude DLB since dementia subtypes may co-exist, with diagnostic overlaps becoming more likely with increasing age and severity.

Imaging of the dopaminergic pathway using SPECT with the I123 presynaptic ligand FP-CIT has proven helpful in diagnosing DLB, where an absence of putamen uptake and reduced uptake in the caudate may be observed. Conversely, healthy controls and AD patients will have good uptake in these regions. Substantia nigra hyperechogenicity is frequently seen in DLB, corticobasal degeneration and hereditary parkinsonism; thus is an unreliable distinguishing feature.[61] In addition, cardiac sympathetic denervation, characterised by a decreased uptake of iodine-123-metaiodobenzylguanidine (MIBG)

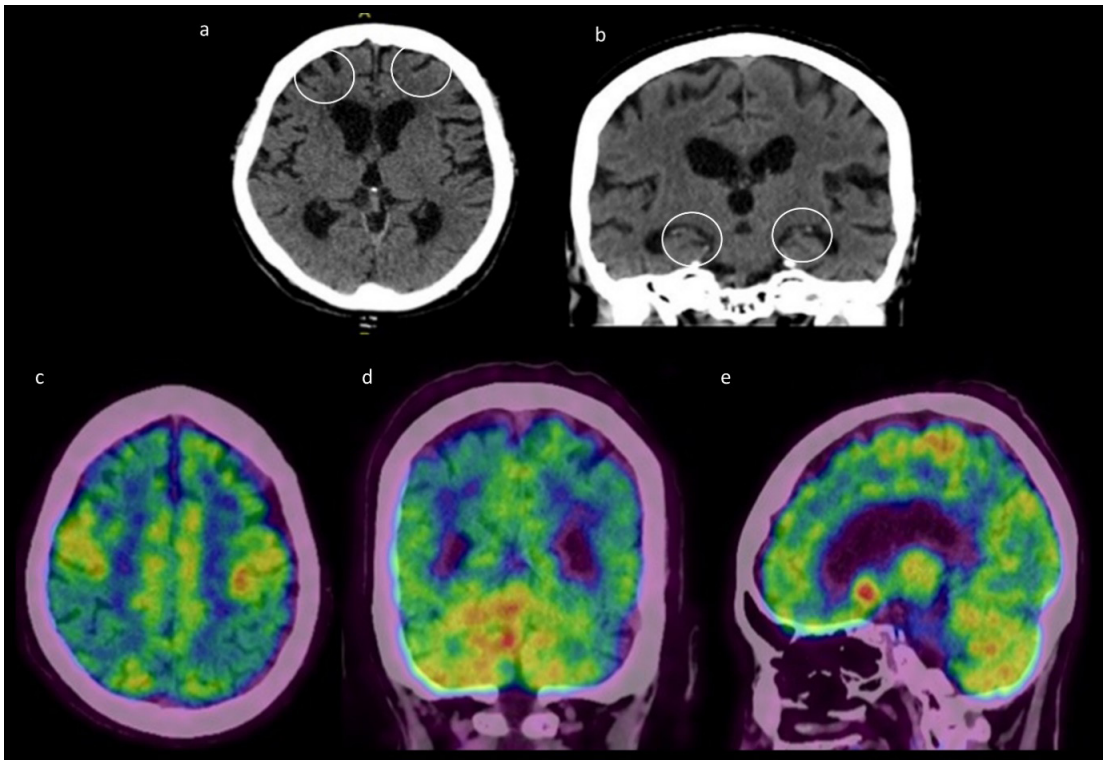

Figure 5. Dementia with Lewy bodies.
Plain CT Brain in (a) axial and (b) coronal showing generalised brain atrophy, more severely affecting the frontal and temporal lobes (circle).
^{18}FDG PET CT co-registered images (c)-(e) demonstrate decreased glucose metabolism in bilateral frontal, parietal, temporal & primary visual cortex

in myocardial scintigraphy, has been detected in DLB and shown to have 98 % sensitivity in differentiating DLB from other dementias.[62]

PARKINSONIAN SYNDROMES

There is often a component of dementia in Parkinsonian syndromes, such as in idiopathic Parkinson's disease (PD) and Parkinson-plus syndromes like progressive supranuclear palsy (PSP) and multisystem atrophy (MSA). PSP often presents with vertical eye movement impairment and postural instability, which causes the sufferers to lose balance and fall. Multiple system atrophy (MSA) usually presents mild cerebellar symptoms, orthostatic hypotension and urinary dysfunction. Loss of the nigrosome 'swallow tail sign' of the substantia nigra on susceptibility weighted imaging (SWI) MRI sequence yields a high diagnostic accuracy for PD (Figure 6).[63]

In addition to MRI, transcranial sonography may be helpful in differentiating Parkinson-plus from PD. Transcranial sonography has been shown to detect increased echogenicity due to iron deposits in deep nuclei such as the substantia nigra, which is useful to differentiate PD from certain atypical Parkinsonian dementias.[64] However, this technique has its drawbacks depending on the thickness of the temporal bones. Normal echogenic substantia nigra indicates the presence of MSA rather than PD. Dilatation of the third-ventricle (>10 mm) and hyperechogenicity at the lenticular nucleus suggests PSP rather than PD.[61]

Significant dorsal midbrain atrophy may be present on MRI of individuals with PSP, especially in the anteroposterior plane and third ventricle dilation. The anteroposterior mid-brain diameter in the mid-sagittal slice is less than 15 mm in individuals with PSP, compared to more than 17 mm in PD and controls.[65] However, smaller mid-brain sizes may also be seen in MSA. While a previous study had suggested that the pons to mid-brain area ratio may completely differentiate PSP from PD and MSA subjects[66], there have been reports of some overlap in subsequent studies. Improvements in measurement capacity in volumetric T1 scan has made it possible to derive the [(P/M) × (MCP/SCP)] index by determining the pons to mid-brain area ratio (P/M) on the

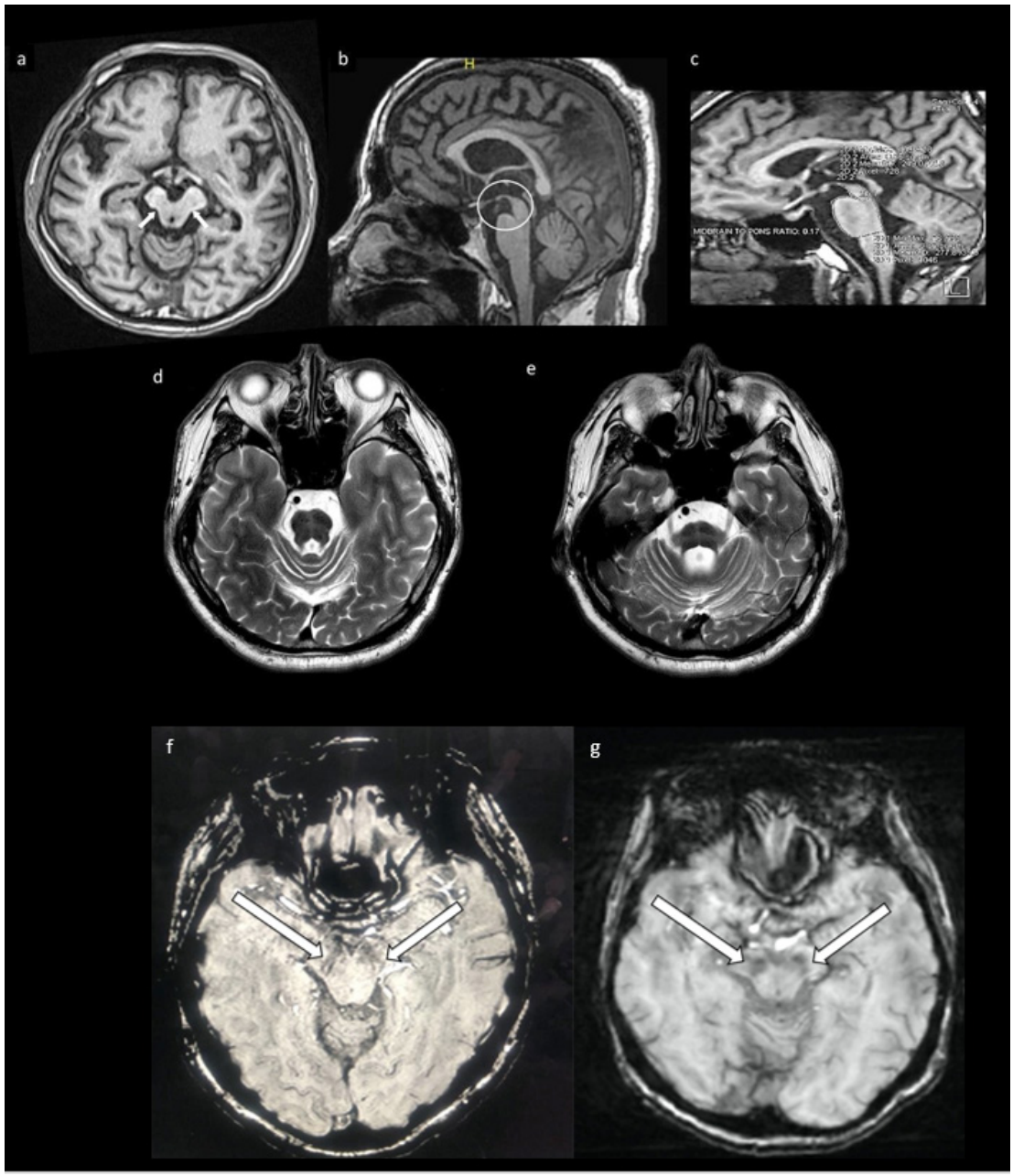

Figure 6. Parkinsonian syndromes - Progressive supranuclear palsy, multisystem atrophy and Parkinson's disease. a) Axial T1W image depicting concave lateral borders (arrows) with reduced midbrain AP diameter giving rise to the 'Mickey Mouse' sign. b) Sagittal T1W image depicting the 'hummingbird sign' (circle) c) Sagittal T1W image which shows the reduced calculated midbrain to pons ratio (0.17), measured using the area of midbrain and pons in the midsagittal plane. d) and e) Axial T2W images in multisystem atrophy showing volume loss of the cerebellum and pons with cruciate hyperintensities giving rise to the 'hot cross bun' sign. f) Axial SWI image of normal healthy control with presence normal high signal nigrosome-1 or 'swallow tail sign' bilaterally. g) Axial SWI image of a patient with Parkinson's disease showing loss of the swallow tail indicating increased iron deposition bilaterally (white arrows).

mid-sagittal section and the middle to superior cerebellar peduncle width ratio (MCP/SCP). This index, also known as the MR Parkinsonism index, can differentiate patients with PSP from those with PD, MSA-P or healthy controls with 100 % sensitivity and specificity in a cohort of

33 patients as there was no overlap of the PSP index (median 19.42) with MSA-P (median 6.53), PD (median 9.40) or controls (median 9.21).[67] MSA is associated with posterolateral putaminal hypointensity (due to iron deposition) with a hyperintense rim, mainly due to gliosis, on T2-weighted imaging. These features are helpful to differentiate MSA from PD with fair accuracy (sensitivity 69%, specificity 97%).[68]

The most common neurodegenerative cerebellar disorders among adults include the cerebellar variant of MSA (MSA-C), idiopathic cerebellar ataxia with (IDCA-P) or without Parkinsonism (IDCA-C), and hereditary spinocerebellar ataxias (SCA). In MSA-C, cerebellar symptoms are more prominent than in Parkinsonism, lower likelihood of cognitive dysfunction.[69] The characteristic cross sign (also called the "hot cross bun" sign) is seen on MRI of patients with MSA-C due to degeneration of transverse pontine fibres. This is associated with middle cerebellar peduncle hyperintensity and pontine atrophy (Figure 6).[70]

Spinocerebellar ataxia (SCA) consists of several subtypes, depending on mutations that define the 28 SCA genotypes, related to differences in cerebral rather than cerebellar involvement.[71] SCA6 is associated with pure cerebellar degeneration on MRI with mild or no cognitive deficits. SCA1 and SCA3 variants display executive dysfunction clinically with putaminal and caudate atrophy on MRI.[72] SCA2 is associated with multiple cognitive domain impairments in approximately a quarter of cases, with both cerebellar and cerebral atrophy apparent on MRI.[73] SCA17 usually presents with Parkinsonism, dystonia, and cognitive dysfunction with cerebral atrophy seen in nearly all cases.[74] The same genotype can present with MSA and PSP like features and have putaminal T2 signal changes that mimic MSA.[75]

Corticobasal degeneration presents with focal dystonia, apraxia or myoclonus, resulting in a "useless arm" or "alien arm sign", progressive asymmetric motor abnormalities, language or speech disturbance, visuospatial deficit or hemineglect.[76] MRI has demonstrated asymmetric frontal and/or parietal atrophy, with less frequent temporal lobe involvement. Left frontoparietal atrophy with the most severe atrophy between superior frontal and precentral sulci has been reported. This area is functionally related to the frontal eye fields.[77] Studies have found that advanced MRI techniques such as high-resolution NODDI are helpful for early diagnosis and monitoring disease progression in PD. Patients with PD have significant reductions in the OD and Vic of the substantia nigra pars compacta and a significant decrease in OD of the putamen.[78] PD is also associated with basal ganglia-thalamocortical network abnormalities on fMRI, EEG or MEG.[9]

CONCLUSION

The role of neuroimaging has evolved immensely and is used to enhance diagnostic capabilities and facililate clinical decisions in many forms of dementia. The salient imaging features of the discussed subtypes of dementia are summarised in Table 2. Recognising specific atrophy patterns, the constellation of clinical features, and particular serum and cerebrospinal fluid biomarkers for the various subtypes of dementia enables more precise diagnosis, prediction of disease progression and

Table 2: Important clinical and imaging features of dementia subtypes

No	Dementia Subtype	Salient Clinical Features	Salient Imaging Features
1	**Alzheimer's disease**	Episodic memory deficit Less language or visual processing difficulties	MRI: Moderate bilateral hippocampal, medial temporal cortex and medial parietal lobe atrophy DTI: reduced FA in cingulum bundle and medial temporal lobe. FDG-PET/HMPAO: reduced cerebral metabolism at the temporoparietal association cortex and posterior cingulate cortex.
2	**Mild cognitive impairment**	Memory deficit not causing ADL impairment	MRI: Mild bilateral hippocampal atrophy Less extensive involvement of the left superior parietal lobule, thalami, anterior cingulate gyrus and temporal lobes DTI: reduced FA in the medial temporal lobe Perfusion: reduced in the right inferior parietal lobe

3	**Vascular Dementia**	Stepwise progression of cognitive decline Predominantly frontal-executive dysfunction compared to memory deficit	Large vessel (MCA) strokes, multiple bilateral smaller ACA or PCA territory infarcts, watershed infarcts, small vessel disease or microhaemorrhages.
4	**Frontotemporal Lobe Degeneration** (Behavioural variant, semantic dementia or progressive non-fluent aphasia subtypes)	Younger patients	Asymmetric frontal and temporal cortical atrophy Atrophy of anterior or entire corpus callosum BvFTD: symmetric frontal lobe atrophy SD: left anterior inferior temporal lobe atrophy PNFA: left perisylvian and frontal atrophy
5	**Dementia with Lewy bodies (DLB)**	Cognitive impairment with executive dysfunction, visuospatial impairment, visual hallucinations, parkinsonian motor features, cognitive fluctuations, rapid eye movement disorder, and severe neuroleptic sensitivity. Dementia symptoms precede motor symptoms	MRI: Global and subcortical volume loss with relatively preserved hippocampi SPECT imaging: absence of putamen uptake, reduced caudate uptake Reduced MIBG uptake in myocardial scintigraphy
6	**Parkinsonian syndromes (Parkinson's disease and Parkinson-plus syndromes such as progressive supranuclear palsy (PSP) and multiple system atrophy (MSA)**	Parkinson's disease – motor symptoms precede dementia PSP – postural instability and vertical eye movement impairment MSA- cerebellar symptoms, orthostatic hypotension and urinary dysfunction Corticobasal degeneration: focal dystonia, apraxia or myoclonus with progressive motor, language, speech, visuospatial deficit or hemineglect	Transcranial ultrasound – PD: increased echogenicity at the substantia nigra PSP: Dilatation of the third ventricle (>10 mm) and hyperechogenicity at the lenticular nucleus MSA: normal echogenicity at the substantia nigra MRI - PD: Loss of swallow tail sign on axial SWI PSP: dorsal midbrain atrophy, high Parkinsonism index (median 19.42 MSA-P: T2W hypointense putamen with a hyperintense rim MSA-C: hot cross bun sign, middle cerebellar peduncle hyperintensity and pontine atrophy Spinocerebellar ataxia: cerebellar degeneration Corticobasal degeneration: asymmetric frontal and/or parietal atrophy most affecting the junction between the superior frontal and precentral sulci

management. Furthermore, this knowledge can be extended to screen for neurodegenerative conditions in at-risk individuals to initiate early treatment and slow disease progression.

DISCLOSURE

Financial support: This work was supported by the Universiti Malaya Postgraduate Research Fund (Grant No: PO076-2015B) and Universiti

Malaya Research Grant Programme (Wellness) Fund (Grant No: RP052B-17HTM).

REFERENCES

1. American Psychiatric Association. Diagnostic and Statistical Manual of Mental Disorders. 4th ed. Washington, DC: American Psychiatric Association, 1994 DOI:10.1001/jama.1994.03520100096046.
2. Prince M, Jackson J. World Alzheimer Report 2009. Alzheimer's Disease International, London (2009). Accessed on 20 August 2021.
3. Knopman DS, DeKosky ST, Cummings JL, *et al*. Practice parameter: diagnosis of dementia (an evidence-based review). Report of the Quality Standards Subcommittee of the American Academy of Neurology. *Neurology* 2001;56(9):1143-53. DOI:10.1212/WNL.56.9.1143.
4. McKiernan EF, O'Brien JT. 7T MRI for neurodegenerative dementias in vivo: a systematic review of the literature. *J Neurol Neurosurg Psychiatry* 2017; 88(7):564-74. DOI: 10.1136/jnnp-2016-315022.
5. Nir TM, Jahanshad N, Villalon-Reina JE, *et al*. Effectiveness of regional DTI measures in distinguishing Alzheimer's disease, MCI, and normal aging. *Neuroimage Clin* 2013;3:180-95. DOI:10.1016/j.nicl.2013.07.006.
6. Zhang H, Schneider T, Wheeler-Kingshott CA, Alexander DC. NODDI: practical in vivo neurite orientation dispersion and density imaging of the human brain. *Neuroimage* 2012;61(4):1000-16. DOI: 10.1016/j.neuroimage.2012.03.072.
7. Faro SH, Mohamed FB, eds. BOLD fMRI: A guide to functional imaging for neuroscientists. Springer Science & Business Media; 2010 Jul 3. DOI 10.1007/978-1-4419-1329-6.
8. Tuladhar AM, van Uden IW, Rutten-Jacobs LC, *et al*. Structural network efficiency predicts conversion to dementia. *Neurology* 2016;86(12):1112-9. DOI: 10.1212/WNL.0000000000002502.
9. Pievani M, de Haan W, Wu T, Seeley WW, Frisoni GB. Functional network disruption in the degenerative dementias. *Lancet Neurol* 2011;10(9):829-43. DOI: 10.1016/S1474-4422(11)70158-2
10. Braak H, Braak E. Morphological criteria for the recognition of Alzheimer's disease and the distribution pattern of cortical changes related to this disorder. *Neurobiol Aging* 1994; 15(3): 355-6; discussion 379-80. DOI: 10.1016/0197-4580(94)90032-9.
11. Gauthier S, Reisberg B, Zaudig M, *et al*. Mild cognitive impairment. *Lancet* 2006; 367(9518): 1262-70. DOI: 10.1016/S0140-6736(06)68542-5.
12. Chow N, Hwang KS, Hurtzet S, *et al*. Comparing 3T and 1.5T MRI for mapping hippocampal atrophy in the Alzheimer's Disease Neuroimaging Initiative. *AJNR Am J Neuroradiol* 2015;36(4):653-60. DOI: 10.3174/ajnr.A4228.
13. Jack CR Jr. Alzheimer disease: new concepts on its neurobiology and the clinical role imaging will play. Radiology 2012; 263(2):344-61. DOI: 10.1148/radiol.12110433.
14. Pennanen C, Testa C, Laakso MP, *et al*. A voxel based morphometry study on mild cognitive impairment. *J Neurol Neurosurg Psychiatry* 2005;76(1):11. DOI:10.1136/jnnp.2004.035600.
15. Meadowcroft MD, Connor JR, Smith MB, Yang QX. MRI and histological analysis of beta amyloid plaques in both human Alzheimer's disease and APP/PS1 transgenic mice. *J Magn Reson Imaging* 2009; 29(5):997-1007. DOI: 10.1002/jmri.21731.
16. Zhang Y, Schuff N, Jahng GH, *et al*. Diffusion tensor imaging of cingulum fibers in mild cognitive impairment and Alzheimer disease. *Neurology* 2007; 68(1):13-9. DOI: 10.1212/01.wnl.0000250326.77323.01.
17. Choo IH, Lee DY, Oh JS, *et al.* Posterior cingulate cortex atrophy and regional cingulum disruption in mild cognitive impairment and Alzheimer's disease. *Neurobiol Aging* 2010;31(5):772-9. DOI: 10.1016/j.neurobiolaging.2008.06.015.
18. Fellgiebel A, Wille P, Müller MJ, *et al*. Ultrastructural hippocampal and white matter alterations in mild cognitive impairment: a diffusion tensor imaging study. *Dement Geriatr Cogn Disord* 2004;18(1):101-8. DOI:10.1159/000077817.
19. Rose SE, McMahon KL, Janke AL, *et al*. Diffusion indices on magnetic resonance imaging and neuropsychological performance in amnestic mild cognitive impairment. *J Neurol Neurosurg Psychiatry* 2006;77(10):1122-8. DOI:10.1136/jnnp.2005.074336.
20. Salat DH, Tuch DS, Van der Kouwe AJ, *et al.* White matter pathology isolates the hippocampal formation in Alzheimer's disease. *Neurobiol Aging* 2010;31(2): 244-56. DOI: 10.1016/j.neurobiolaging.2008.03.013.
21. Zhou Y, Dougherty Jr JH, Hubner KF, Bai B, Cannon RL, Hutson RK. Abnormal connectivity in the posterior cingulate and hippocampus in early Alzheimer's disease and mild cognitive impairment. *Alzheimer Dement* 2008;4(4):265-70. DOI: 10.1016/j.jalz.2008.04.006.
22. Bozzali M, Falini A, Franceschi M, *et al*. White matter damage in Alzheimer's disease assessed in vivo using diffusion tensor magnetic resonance imaging. *J Neurol Neurosurg Psychiatry* 2002;72(6):742-6. DOI: 10.1136/jnnp.72.6.742.
23. Kavcic V, Ni H, Zhu T, Zhong J, Duffy CJ. White matter integrity linked to functional impairments in aging and early Alzheimer's disease. *Alzheimer Dement* 2008;4(6):381-9 DOI: 10.1016/j.jalz.2008.07.001.
24. Petrella JR, Coleman RE, Doraiswamy PM, Neuroimaging and early diagnosis of Alzheimer disease: a look to the future. *Radiology* 2003;226(2):315-36. DOI: 10.1148/radiol.2262011600.
25. Klunk WE, Engler H, Nordberg A, *et al*. Imaging brain amyloid in Alzheimer's disease with Pittsburgh Compound-B. *Ann Neurol* 2004;55(3):306-19. DOI: 10.1002/ana.20009.
26. Wong DF, Rosenberg PB, Zhou Y, *et al*. In vivo imaging of amyloid deposition in Alzheimer disease using the radioligand 18F-AV-45 (flobetapir F 18). *J Nucl Med* 2010;51(6): 913-20. DOI: 10.2967/jnumed.109.069088.

27. Johnson NA, Jahng GH, Weiner MW, *et al*. Pattern of cerebral hypoperfusion in Alzheimer disease and mild cognitive impairment measured with arterial spin-labeling MR imaging: initial experience. *Radiology* 2005;234(3):851-9. DOI: 10.1148/radiol.2343040197.
28. Greicius MD, Srivastava G, Reiss AL, Menon V. Default-mode network activity distinguishes Alzheimer's disease from healthy aging: evidence from functional MRI. *Pro Natl Acad Sci U S A* 2004;101(13):4637-42. DOI: 10.1073/pnas.0308627101.
29. Rombouts SA, Barkhof F, Goekoop R, Stam CJ, Scheltens P. Altered resting state networks in mild cognitive impairment and mild Alzheimer's disease: an fMRI study. *Hum Brain Mapp* 2005;26(4):231-9. DOI:10.1002/hbm.20160.
30. Varatharajah Y, Ramanan VK, Iyer R, Vemuri P. Predicting short-term MCI-to-AD progression using imaging, CSF, genetic factors, cognitive resilience, and demographics. *Sci Rep* 2019;9(1):1-5. DOI: 10.1038/s41598-019-38793-3.
31. Korolev IO, Symonds LL, Bozoki AC, Alzheimer's Disease Neuroimaging Initiative. Predicting progression from mild cognitive impairment to Alzheimer's dementia using clinical, MRI, and plasma biomarkers via probabilistic pattern classification. *PloS One* 2016;11(2):e0138866. DOI: 10.1371/journal.pone.0138866.
32. Stebbins GT, Murphy CM. Diffusion tensor imaging in Alzheimer's disease and mild cognitive impairment. *Behav Neurol* 2009. 21(1-2): 39-49. DOI: 10.3233/BEN-2009-0234.
33. Amlien IK, Fjell AM. Diffusion tensor imaging of white matter degeneration in Alzheimer's disease and mild cognitive impairment. *Neuroscience* 2014; 276: 206-15. DOI: 10.1016/j.neuroscience.2014.02.017.
34. Binnewijzend MA, Kuijer JP, Benedictus MR, *et al*. Cerebral blood flow measured with 3D pseudocontinuous arterial spin-labeling MR imaging in Alzheimer disease and mild cognitive impairment: a marker for disease severity. *Radiology* 2013;267(1):221-30. DOI: 10.1148/radiol.12120928.
35. Ding B, Ling HW, Zhang Y, *et al*. Pattern of cerebral hyperperfusion in Alzheimer's disease and amnestic mild cognitive impairment using voxel-based analysis of 3D arterial spin-labeling imaging: initial experience. *Clin Interv Aging* 2014;9:493. DOI: 10.2147/CIA.S58879.
36. Alexopoulos P, Sorg C, Förschler A, *et al*. Perfusion abnormalities in mild cognitive impairment and mild dementia in Alzheimer's disease measured by pulsed arterial spin labeling MRI. *Eur Arch Psychiatr Clin Neurosci* 2012; 262(1):69-77. DOI: 10.1007/s00406-011-0226-2.
37. Korczyn AD, Vakhapova V, Grinberg LT. Vascular dementia. *J Neurol Sci* 2012; 15;322(1-2):2-10. DOI: 10.1016/j.jns.2012.03.027.
38. Vitali P, Migliaccio R, Agosta F, Rosen HJ, Geschwind MD. Neuroimaging in dementia. *Semin Neurol* 2008; 28(4): 467-83. DOI: 10.1055/s-0028-1083695.
39. Guermazi A, Miaux Y, Rovira-Cañellas A, *et al.* Neuroradiological findings in vascular dementia. *Neuroradiology* 2007; 49(1):1-22. DOI: 10.1007/s00234-006-0156-2.
40. Hugues C, Joutel A, Dichgans M, Tournier-Lasserve E, Bousser MG. Cadasil. *Lancet Neurol* 2009; 8(7): 643-53. DOI: 10.1016/S1474-4422(09)70127-9.
41. Roman GC, Erkinjuntti T, Wallin A. Pantoni L, Chui HC. Subcortical ischaemic vascular dementia. *Lancet Neurol* 2002;1(7): 426-36. DOI: 10.1016/S1474-4422(02)00190-4.
42. McKhann GM, Knopman DS, Chertkow H, *et al*. The diagnosis of dementia due to Alzheimer's disease: Recommendations from the National Institute on Aging-Alzheimer's Association workgroups on diagnostic guidelines for Alzheimer's disease. *Alzheimer Dement* 2011; 7(3):263-9. DOI: 10.1016/j.jalz.2011.03.005.
43. Bhogal P, Mahoney C, Graeme-Baker S, Roy A, *et al*. The common dementias: a pictorial review. *Eur Radiol* 2013; 23(12):3405-17. DOI: 10.1007/s00330-013-3005-9.
44. Cordonnier C, Van der Flier WM, Sluimer JD, Leys D, Barkhof F, Scheltens PH. Prevalence and severity of microbleeds in a memory clinic setting. *Neurology* 2006; 66(9):1356-60. DOI: 10.1212/01.wnl.0000210535.20297.ae.
45. Koennecke HC. Cerebral microbleeds on MRI: prevalence, associations, and potential clinical implications. *Neurology* 2006; 66(2):165-71. DOI: 10.1212/01.wnl.0000194266.55694.1e.
45. Lee SH, Kim SM, Kim N, Yoon BW, Roh JK. Cortico-subcortical distribution of microbleeds is different between hypertension and cerebral amyloid angiopathy. *J Neurol Sci* 2007; 258(1-2):111-4. DOI: 10.1016/j.jns.2007.03.008.
47. Bastos-Leite AJ, Kuijer JP, Rombouts SA, *et al*. Cerebral blood flow by using pulsed arterial spin labeling in elderly subjects with white matter hyperintensities. *Am J Neuroradiol* 2008; 29(7):1296-301. DOI: 10.3174/ajnr.A1091.
48. Mackenzie IR, Neumann M, Bigio EH, *et al*. Nomenclature for neuropathologic subtypes of frontotemporal lobar degeneration: consensus recommendations. *Acta Neuropathol* 2009; 117(1): 15-8. DOI: 10.1007/s00401-008-0460-5.
49. Josephs KA. Frontotemporal lobar degeneration. *Neurol Clin* 2007; 25(3):683-696. DOI: 10.1016/j.ncl.2007.03.005.
50. Kitagaki H, Mori E, Yamaji S, *et al*. Frontotemporal dementia and Alzheimer disease: evaluation of cortical atrophy with automated hemispheric surface display generated with MR images. *Radiology* 1998; 208(2): 431-9. DOI: 10.1148/radiology.208.2.9680572.
51. Yamauchi H, Fukuyama H, Nagahama Y, *et al*. Comparison of the pattern of atrophy of the. corpus callosum in frontotemporal dementia, progressive supranuclear palsy, and Alzheimer's disease. *J Neurol Neurosurg Psychiatry* 2000; 69(5): 623-9. DOI: 10.1136/jnnp.69.5.623.
52. Kipps CM, Davies RR, Mitchell J, Kril JJ, Halliday GM, Hodges JR. Clinical significance of lobar atrophy in frontotemporal dementia: application of an MRI visual rating scale. *Dement Geriatr Cogn Disord* 2007;23(5):334-42. DOI: 10.1159/000100973.

53. Talbot PR, Lloyd JJ, Snowden JS, Neary D, Testa HJ. A clinical role for 99mTc-HMPAO SPECT in the investigation of dementia? *J Neurol Neurosurg Psychiatry* 1998; 64(3): 306-13. DOI: 10.1136/jnnp.64.3.306.
54. Zhang Y, Schuff N, Du AT, *et al*. White matter damage in frontotemporal dementia and Alzheimer's disease measured by diffusion MRI. *Brain* 2009; 32(9): 2579-92. DOI: 10.1093/brain/awp071.
55. Rabinovici GD, Furst AJ, O'neil JP, *et al*. 11C-PIB PET imaging in Alzheimer disease and frontotemporal lobar degeneration. *Neurology* 2007; 68(15):1205-12.
56. Du AT, Jahng GH, Hayasaka S, *et al*. Hypoperfusion in frontotemporal dementia and Alzheimer disease by arterial spin labeling MRI. *Neurology* 2006; 67(7):1215-20. DOI: 10.1212/01.wnl.0000238163.71349.78.
57. Marshall VL, Patterson J, Hadley DM, Grosset KA, Grosset DG. Two-year follow-up in 150 consecutive cases with normal dopamine transporter imaging. *Nucl Med Commun* 2006; 27(12): 933-7. DOI: 10.1097/01.mnm.0000243374.11260.5b.
58. Zhou J, Greicius MD, Gennatas ED, *et al*. Divergent network connectivity changes in behavioural variant frontotemporal dementia and Alzheimer's disease. *Brain* 2010; 133(5): 1352-67. DOI: 10.1093/brain/awq075.
59. McKeith IG, DD LJ, Emre M, O'brien JT, *et al*. Diagnosis and management of dementia with Lewy bodies: third report of the DLB Consortium. *Neurology* 2005; 65(12): 1863-72. DOI: 10.1212/01.wnl.0000187889.17253.b1.
60. Burton EJ, Karas G, Paling SM, *et al*. Patterns of cerebral atrophy in dementia with Lewy bodies using voxel-based morphometry. *Neuroimage* 2002; 17(2): 618-30. DOI: 10.1006/nimg.2002.1197.
61. Walter U, Dressler D, Probst T, *et al*. Transcranial brain sonography findings in discriminating between parkinsonism and idiopathic Parkinson disease. *Arch Neurol* 2007; 64(11): 1635-40. DOI: 10.1001/archneur.64.11.1635.
62. Treglia G, Cason E. Diagnostic performance of myocardial innervation imaging using MIBG scintigraphy in differential diagnosis between dementia with lewy bodies and other dementias: a systematic review and a meta-analysis. *J Neuroimaging* 2012; 22(2): 111-7. DOI:10.1111/j.1552- 6569.2010.00532.x.
63. Schwarz ST, Afzal M, Morgan PS, Bajaj N, Gowland PA, Auer DP. The 'swallow tail'appearance of the healthy nigrosome–a new accurate test of Parkinson's disease: a case-control and retrospective cross-sectional MRI study at 3T. *PloS One* 2014; 7;9(4):e93814. DOI: 10.1371/journal.pone.0093814.
64. Berg D. Disturbance of iron metabolism as a contributing factor to SN hyperechogenicity in Parkinson's disease: implications for idiopathic and monogenetic forms. *Neurochem Res* 2007; 32(10): 1646-54. DOI: 10.1007/s11064-007-9346-5.
65. Warmuth-Metz M, Naumann M, Csoti I, Solymosi L. Measurement of the midbrain diameter on routine magnetic resonance imaging: a simple and accurate method of differentiating between Parkinson disease and progressive supranuclear palsy. *Arch Neurol* 2001; 58(7):1076-9. DOI:10.1001/archneur.58.7.1076.
66. Oba H, Yagishita A, Terada H, *et al*. New and reliable MRI diagnosis for progressive supranuclear palsy. *Neurology* 2005; 64(12): 2050-5. DOI: 10.1212/01.WNL.0000165960.04422.D0.
67. Quattrone A, Nicoletti G, Messina D, *et al*. MR imaging index for differentiation of progressive supranuclear palsy from Parkinson disease and the Parkinson variant of multiple system atrophy. *Radiology* 2008; 246(1):214-21. DOI: 10.1148/radiol.2453061703.
68. von Lewinski F, Werner C, Jörn T, Mohr A, Sixel-Döring F, Trenkwalder C. T2*-weighted MRI in diagnosis of multiple system atrophy. *J Neurol* 2007; 254(9):1184-8. DOI: 10.1007/s00415-006-0496-1.
69. Bürk K, Daum I, Rüb U. Cognitive function in multiple system atrophy of the cerebellar type. *Mov Disord* 2006; 21(6): 772-6. DOI: 10.1002/mds.20802.
70. Abe K, Hikita T, Yokoe M, Mihara M, Sakoda S. The "cross" signs in patients with multiple system atrophy: a quantitative study. *J Neuroimaging* 2006; 16(1): p. 73-7. DOI: 10.1177/1051228405279988
71. Burk K. Cognition in hereditary ataxia. C*erebellum* 2007; 6(3):280-6. DOI:10.1080/14734220601115924
72. Klockgether T, Skalej M, Wedekind D, *et al*. Autosomal dominant cerebellar ataxia type I. MRI based volumetry of posterior fossa structures and basal ganglia in spinocerebellar ataxia types 1, 2 and 3. *Brain* 1998; 121(9): 1687-93. DOI: 10.1093/brain/121.9.1687
73. Brenneis C, Bösch SM, Schocke M, Wenning GK, Poewe W. Atrophy pattern in SCA2 determined by voxel-based morphometry. *Neuroreport* 2003; 14(14): 1799-802. DOI: 10.1097/00001756-200310060-00008
74. Mariotti C, Alpini D, Fancellu R, *et al*. Spinocerebellar ataxia type 17 (SCA17): oculomotor phenotype and clinical characterization of 15 Italian patients. *J Neurol* 2007; 254(11): 1538-46. DOI: 10.1007/s00415-007-0579-7
75. Josephs KA, Whitwell JL, Knopman DS, *et al*. Two distinct subtypes of right temporal variant frontotemporal dementia. *Neurology* 2009; 73(18): 1443-50. DOI:10.1212/WNL.0b013e3181bf9945
76. Litvan I, Agid Y, Goetz C, *et al*. Accuracy of the clinical diagnosis of corticobasal degeneration: aclinicopathologic study. *Neurology* 1997; 48(1): 119-25. DOI: 10.1212/WNL.48.1.119.
77. Boxer AL, Geschwind MD, Belfor N, *et al*. Patterns of brain atrophy that differentiate corticobasal degeneration syndrome from progressive supranuclear palsy. *Arch Neurol* 2006; 63(1):81-6. DOI:10.1001/archneur.63.1.81
78. Kamagata K, Hatano T, Okuzumi A, *et al*. Neurite orientation dispersion and density imaging in the substantia nigra in idiopathic Parkinson disease. *Eur Radiol* 2016; 26(8): 2567-77. DOI: 10.1007/s00330-015-4066-8